



# Exosomes derived from human exfoliated deciduous teeth ameliorate adult bone loss in mice through promoting osteogenesis

Jizhen Wei<sup>1,2</sup> · Yeqing Song<sup>2</sup> · Zhihao Du<sup>2</sup> · Feiyan Yu<sup>3</sup> · Yimei Zhang<sup>4</sup> · Nan Jiang<sup>2</sup> · Xuejun Ge<sup>1</sup>

Received: 15 February 2020 / Accepted: 6 July 2020 / Published online: 12 July 2020  
© Springer Nature B.V. 2020

## Abstract

Cell-free based therapy is an effective strategy in regenerative medicine as it avoids controversial issues, such as immunomodulation and stability. Recently, exosomes have been explored as a favorable substitution for stem cell therapy as they exhibit multiple advantages, such as the ability to be endocytosed and innate biocompatibility. This study aimed to investigate the effects of stem cells from human exfoliated deciduous teeth (SHED)-derived exosomes (SHED-Exo) on bone marrow stromal cells (BMSCs) osteogenesis and bone recovery. SHED-Exo were isolated, characterized, and applied to the bone loss area caused by periodontitis in a mouse model. We found that the injection of SHED-Exo restored bone loss to the same extent as original stem cells. Without affecting BMSCs proliferation, SHED-Exo mildly inhibited apoptosis. Moreover, SHED-Exo specifically promoted BMSCs osteogenesis and inhibited adipogenesis compared with SHED-derived conditioned medium. The expression of osteogenic marker genes, alkaline phosphatase activity, and Alizarin Red S staining of BMSCs was significantly increased by co-culturing with SHED-Exo. Moreover, Western blot analysis showed that Runx2, a key transcriptional factor in osteogenic differentiation, and p-Smad5 were upregulated upon SHED-Exo stimulation. Expression of the adipogenic marker *PPAR $\gamma$*  and the amount of lipid droplets decreased when exosomes were present. Low doses of exosomes inhibited the expression of the inflammatory cytokines IL-6 and TNF- $\alpha$ . In conclusion, SHED-Exo directly promoted BMSCs osteogenesis, differentiation, and bone formation. Therefore, exosomes have the potential to be utilized in the treatment of periodontitis and other bone diseases.

**Keywords** Stem cells from human exfoliated deciduous teeth (SHED) · Exosomes · Conditioned medium · Osteogenesis · Bone loss

**Electronic supplementary material** The online version of this article (<https://doi.org/10.1007/s10735-020-09896-3>) contains supplementary material, which is available to authorized users.

✉ Nan Jiang  
nanjiang@bjmu.edu.cn

✉ Xuejun Ge  
gxj19722003@163.com

<sup>1</sup> Department of Periodontics, Shanxi Medical University School and Hospital of Stomatology, Taiyuan, Shanxi, China

<sup>2</sup> Central Laboratory, Peking University School and Hospital of Stomatology, #22 Zhongguancun South Avenue, Haidian District, Beijing 100081, China

<sup>3</sup> Department of Oral Medicine, Shanxi Medical University School and Hospital of Stomatology, Taiyuan, Shanxi, China

<sup>4</sup> First Dental Center, Peking University School and Hospital of Stomatology, Beijing, China

## Introduction

Mesenchymal stem cells and progenitor cells of skeletal tissue have been proved to be fundamental tools to restore the loss of bone tissues caused by trauma, inflammation, and aging (Bianco et al. 2013). Stem cells from human-exfoliated deciduous teeth (SHED), which have been identified as a unique type of mesenchymal stem cells with strong proliferative and multi-differentiation capabilities (Miura et al. 2003a), are an ideal post-natal cell source for regenerative medicine (Taguchi et al. 2019). They have been demonstrated to maintain their neurogenic, adipogenic, osteogenic, and odontogenic differentiation potentials (Miura et al. 2003b), which are not even affected by cryopreservation (Lee et al. 2015; Ma et al. 2012). Because of the convenient accessibility of SHED (they can be obtained when alternation of primary and permanent teeth occurs before adolescence), they have been considered as a potential source

of cell therapy. However, the use of mesenchymal stem cells in transplantation is controversial due to their unclear immunomodulatory mechanisms, paracrine modulation, and effects on dying cells (Bianco et al. 2013; Haniffa et al. 2009). Therefore, further experiments are needed to overcome these challenges.

Exosomes, which have a mean diameter of 40–160 nm, mediate cell–cell communication and are secreted by virtually all cells (Mathieu et al. 2019). They participate in organ homeostasis and disease through multiple biological and pathological functions and pathways. As a result, not only their diagnostic, but also their therapeutic potential has been investigated (Fitts et al. 2019; Kalluri and LeBleu 2020). The use of bone marrow mesenchymal stem cell-derived exosomes has emerged as a therapeutic approach for cardiovascular protection (Yuan et al. 2018). Human mesenchymal stem cell-derived exosomes have been reported to promote chondrogenesis and suppress cartilage degradation, and may therefore serve as an osteoarthritis drug (Mao et al. 2018). SHED have strong proliferative and multi-differentiation capabilities and immunosuppressive abilities, but it remains to be elucidated whether their secreted exosomes carry the same advantages and whether they could be applied in tissue regeneration and cell transplantation.

In this study, we: (i) investigated the effects of SHED-derived exosomes (SHED-Exo) in the treatment of inflammation-induced bone loss in a murine periodontitis model and (ii) compared these effects with those of their cells of origin. The effects of SHED-Exo on the proliferation and multi-differentiation abilities of bone marrow stromal cell (BMSCs) were examined *in vitro*, as well as their inflammation modulatory effects. Our findings improve our understanding of the mechanisms underlying the effects of SHED and SHED-Exo on bone formation and provide a foundation for future studies aiming to develop or ameliorate cell-free based therapy.

## Materials and methods

### Animals and cell culture

Male CD-1 mice (9–10 months old) were purchased from Peking University Health Science Center. Periodontitis was induced by silk ligature as previously reported (Abe and Hajishengallis 2013). Briefly, the first molar of the upper jaw was tied with a 5–0 silk ligature (Jinhuan, China) for 14 days. Our experimental protocol was approved by the Ethics Committee of Peking University School of Stomatology (Approval number: LA2019148).

SHED were provided by the Oral Stem Cell Bank of Beijing, Tason Biotech Co., Ltd. and cultured in DMEM (Gibco, MA, USA) with 10% fetal bovine serum (Gibco)

and 1% penicillin/streptomycin (Gibco). Bone marrow stromal cells (BMSCs) were isolated from femur and tibia bone marrow of CD-1 mice (9–10 months old). The mouse bone marrow cells were flushed from long bones with 2% fetal bovine serum (FBS) in PBS. All cells were passed through a 40- $\mu$ m strainer (BD Falcon, USA) to obtain a single-cell suspension. Cells were seeded in 60-mm cell culture dishes with  $\alpha$ -modified essential medium ( $\alpha$ -MEM, Gibco, MA, USA) with 10% FBS (Gibco) and 1% penicillin/streptomycin (Gibco) at 37 °C in 5% CO<sub>2</sub>. After 2 days, cells were washed with PBS to exclude the non-adherent cells. The attached cells were cultured for another 10–12 days. Primary cells were passaged and applied for studies.

### Preparation of SHED-derived exosomes and conditioned medium

SHED were seeded into 10-cm dishes with cell density of  $2 \times 10^5$ /ml in DMEM with 10% fetal bovine serum and 1% penicillin/streptomycin. Passage 4 to 7 SHED was used for exosomes collection (Du et al. 2018). When the cells reached 70% confluence, culture medium was changed to serum-free DMEM with 1% penicillin/streptomycin for 24 h. The supernatant was collected and centrifuged at  $300 \times g$  for 10 min, and the supernatant was collected and centrifuged at  $2000 \times g$  for 10 min. Upon removing non-adherent cells and debris, conditioned medium was collected and named SHED-CM. SHED-CM and BMSCs culture medium were mixed as 1:1 and treated BMSCs in the following experiments. Extracellular vesicles were further purified by ultracentrifugation as previously reported (Jiang et al. 2017). Ultracentrifugation was performed as follows. The supernatant was centrifuged at  $10,000 \times g$  for 60 min. The supernatant was filtered through a 0.22- $\mu$ m filter (Millipore) to remove microvesicles (Catalano and O'Driscoll 2020) and ultracentrifuged (Beckman Coulter, USA) at  $100,000 \times g$  for 70 min. The pellet was washed with PBS to eliminate contamination of proteins and centrifuged again at  $100,000 \times g$  for 70 min. The pellet (extracellular vesicles) was resuspended in PBS and characterized by transmission electron microscopy (TEM) and Western blot analysis.

### Transmission electron microscopy

Exosomes were collected and fixed in 2% paraformaldehyde (PFA), washed, and loaded onto formvar/carbon-coated grids. After washing, exosomes were post-fixed in 2% glutaraldehyde for 2 min and contrasted in 2% phosphotungstic acid for 5 min. Samples were washed, dried, and examined by TEM (JEM-1400, Japan).

## Western blot

To detect exosomal proteins, total protein was extracted from cell lysates, supernatants, and secreted exosomes. Proteins were separated by SDS-PAGE and transferred to a nitrocellulose membrane (Millipore), which was probed with anti-CD63 (1:500, Santa Cruz Biotechnology) and anti-GM130 (1:250, Abcam).

To measure the levels of endogenous proteins, cells were lysed in RIPA buffer (Thermo Scientific, Rockford, IL), and lysate proteins (20 µg per lane) were separated by 4–12% SDS-PAGE and transferred to a nitrocellulose or PVDF membrane (Invitrogen), which was probed with anti-GAPDH (1:1000, Proteintech) and anti-runt-related transcription factor 2 (*Runx2*) (1:250, Abcam), anti-phospho-Smad1/Smad5/Smad9 (1:500, Cell Signaling Technology) and Smad5 (1:500, Cell Signaling Technology). IRDye® 800CW Secondary Antibodies (1:10,000, LI-COR, Lincoln, NE) were applied for 60 min. The signals were detected with an Odyssey® Imaging System.

## Proliferation and multi-lineage differentiation of mouse BMSCs

Mouse BMSCs ( $1 \times 10^4$ /well) were seeded on a 96-well plate (Nunc, USA) and treated with exosomes, conditioned medium, or PBS. Cell proliferation was analyzed with a CCK-8 reagent (APEX BIO, USA) following the manufacturer's instructions. Experiments were performed in triplicate.

For osteogenic differentiation, passage one BMSCs were cultured to confluence for 1–2 weeks in 10 mM β-glycerophosphate, 100 µM L-ascorbic acid 2-phosphate, and 10 nM dexamethasone (Sigma), in the presence of SHED-Exo, SHED-CM, or PBS. Alkaline phosphatase activity was examined using p-Nitrophenyl Phosphate Liquid Substrate (Sigma). Cells were stained with 1% Alizarin Red S (Sigma) to detect mineral nodules after fixed with 4% PFA. For adipogenic differentiation, passage 1 BMSCs were treated with adipogenic differentiation medium (Cytogen, Sunnyvale, CA, USA) and cultured to confluence for 2 weeks. Cells were fixed with 4% PFA and stained with Oil Red O. Total RNA was extracted from at least three independent samples for assaying osteogenesis and adipogenesis markers by quantitative reverse-transcription PCR (qRT-PCR).

## Apoptosis and flow cytometry

BMSCs ( $1 \times 10^5$ /well) were seeded on a 6-well culture plate (Nunc). When cells reached 70% confluence, they were pretreated with SHED-Exo, SHED-CM, or PBS for 24 h. To induce apoptosis, 5 µM camptothecin was added to the cells for 3 h. Cells were stained following the FITC Annexin V

Staining Protocol (BD Bioscience, USA) to measure apoptosis by flow cytometry. Briefly, cells were gently trypsinized, washed twice with cold PBS, and then incubated with 5 µl of FITC Annexin V and 5 µl PI for 15 min at room temperature in the dark. Apoptosis was analyzed by flow cytometry within 1 h.

## qRT-PCR

Total RNA was isolated using TRIzol (Invitrogen) following the manufacturer's protocol. Complementary DNA (cDNA) was synthesized using a cDNA reverse transcription synthesis kit (Invitrogen). qRT-PCR was performed using SYBR Green Master Mix on an ABI Prism 7500 Real-Time PCR system (Applied Biosystems). All of the reactions were run in triplicate. Primers for *Alp*, *Runx2*, *Osx*, *PPARγ*, *TNF-α*, *IL-6*, and *Gapdh* are listed in Table 1. mRNA levels were normalized to *Gapdh*.

## Animal surgery and tissue preparation

After removing the silk ligature, SHED ( $1 \times 10^6$ ), SHED-Exo (20 µg), or PBS were injected into the buccal and lingual sides of the first molar once per week. After 2 weeks, the mice were sacrificed. All of the samples were harvested and immersed in 4% PFA for 24 h, followed by micro-CT and histology preparation.

The harvested upper jaw specimens were scanned by micro-CT (Siemens). All of the specimens were placed and scanned with the same setup parameters (pixel size, 8.99 µm; voltage, 80 kV; current, 500 µA; exposure time, 1.500 s). The 3D images were reconstructed with Inveon Research Workplace 3.0 software (Siemens), and relevant

**Table 1** Real-time PCR primers

Genes	Primers
<i>Gapdh</i>	Forward 5'–3': aacgacccttcattgacctc Reverse 5'–3': actgtgccgttgaaattgcc
<i>Runx2</i>	Forward 5'–3': atgatggtgtgacgctgac Reverse 5'–3': tcaatatggccccaacag
<i>Alp</i>	Forward 5'–3': ccaactcttttgccagaga Reverse 5'–3': ggctacattggtgtgagcttt
<i>Osx</i>	Forward 5'–3': tcctggatagactcatcctc Reverse 5'–3': ccaaggtagtaggtgtgtgccc
<i>PPARγ</i>	Forward 5'–3': ttcaagggtgccagtttcg Reverse 5'–3': acttgagcagatcacttggtc
<i>IL-6</i>	Forward 5'–3': acaaagccagagtccttcagag Reverse 5'–3': ttgacctctctgtgactc
<i>TNF-α</i>	Forward 5'–3': cacactcacaaccaccaagtg Reverse 5'–3': ttgagatccatgccgttg

distances were calculated. Each group included at least four samples for analysis.

After scanning, specimens were prepared for decalcification in 0.5 M EDTA (pH 7.4) for 14–21 days, embedded in paraffin, and cut into 5- $\mu$ m sections. Randomly selected sections were used for H&E staining and Masson trichrome staining using a kit (Zhongshan Golden Bridge Biotechnology, China) for bone formation analysis. Immunohistochemistry was performed using a two-step detection kit (Zhongshan Golden Bridge Biotechnology). Briefly, specimens were applied in antigen retrieval solution for 10 min, blocked with 5% bovine serum albumin (BSA) for 30 min, and incubated with primary antibody against TNF- $\alpha$  (1:100, santa cruz) overnight at 4 °C. On the second day, after rinsing thoroughly in PBS, the horseradish peroxidase-conjugated secondary antibody (Zhongshan Golden Bridge Biotechnology) was dropped onto slides. The defect area of each slide was observed using a Zeiss light microscope.

### Statistical analysis

All of the quantitative data were analyzed using ImageJ. After confirming data were normally distributed, data were analyzed by one-way ANOVA followed by Tukey's post hoc test. Differences were considered statistically significant if  $P \leq 0.05$ .

## Results

### Isolation and characterization of SHED-Exo

We isolated SHED and SHED-Exo and explored their morphology and the levels of exosomal markers. Passage 4–7 cells were used for experiments. They maintained a homogeneous spindle-like morphology (Fig. 1a) and sustained a stable growth rate and stable protein levels (Du et al. 2018). SHED-Exo were harvested by ultracentrifugation from culture medium and identified by TEM and western blot. TEM revealed that collected extracellular vesicles were ~100 nm

in diameter and had a spherical and membrane-encapsulated structure (Fig. 1b) typical of exosomes. Harvested vesicles were positive for CD63, but negative for the Golgi marker GM130, as shown by Western blot analysis (Fig. 1c). These results show that SHED-Exo had exosomal characteristics (Zhang et al. 2015).

### Exosomes rescued ligature-induced periodontitis bone loss in mice

To assess whether SHED-Exo have comparable effects on bone metabolism as their cells of origin, we used a periodontitis mouse model (induced by silk ligature around the first molar for 14 days) (Fig. 2a). After 14 days of ligature stimulation, severe alveolar bone loss was observed by micro-CT on both the buccal and the lingual side (Fig. 2b). After removing the ligature, we injected SHED-Exo, SHED, or PBS into the mesial and distal spaces of the molar once a week ( $n = 4–6$ ). SHED and SHED-Exo significantly increased the bone height, while PBS did not. Furthermore, we examined the distance from the cemento-enamel junction (CEJ) to the alveolar bone crest in the sagittal view. In Fig. 2c, the red line indicates the bone loss height. PBS could not restore the alveolar bone height; more severe bone loss was observed in the control group. In the SHED and SHED-Exo groups, the bone loss height was significantly decreased compared with the PBS group. In both groups, at the distal site, the alveolar bone height nearly reached the healthy unligatured level. Although the average alveolar bone crest height was higher in the SHED group than in the SHED-Exo group, this difference was not statistically significant (Fig. 3a). SHED and SHED-Exo could both decrease the bone loss distance at the first molar mesial site; however, there was no significant difference between different treatment groups (Fig. 3b).

To further examine the histology of alveolar bone regeneration structures, the area between the first and second molars (M1 and M2) was stained. H&E staining showed an alveolar bone outline, marked by a black dotted line. After inducing periodontitis, the amount of alveolar bone from

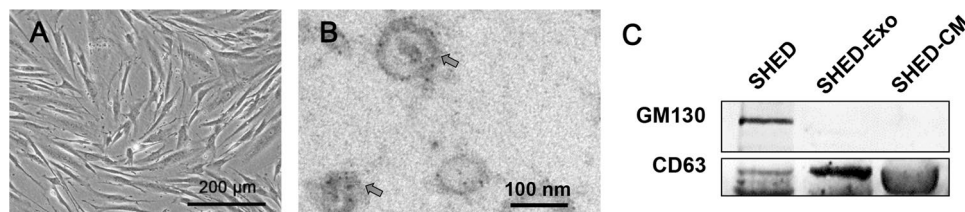


**Fig. 1** Characterization of SHED-Exo. **a** SHED were cultured to passage 4–7 and had a typical spindle-like cell morphology. **b** The isolated extracellular particles in culture medium, examined by transmission electron microscopy, showing a membrane-encapsulated

structure with a diameter of ~100 nm. The arrow indicates SHED-Exo. **c** Western blot analysis of total proteins isolated from parent cells, vesicles, and exosome-free culture medium



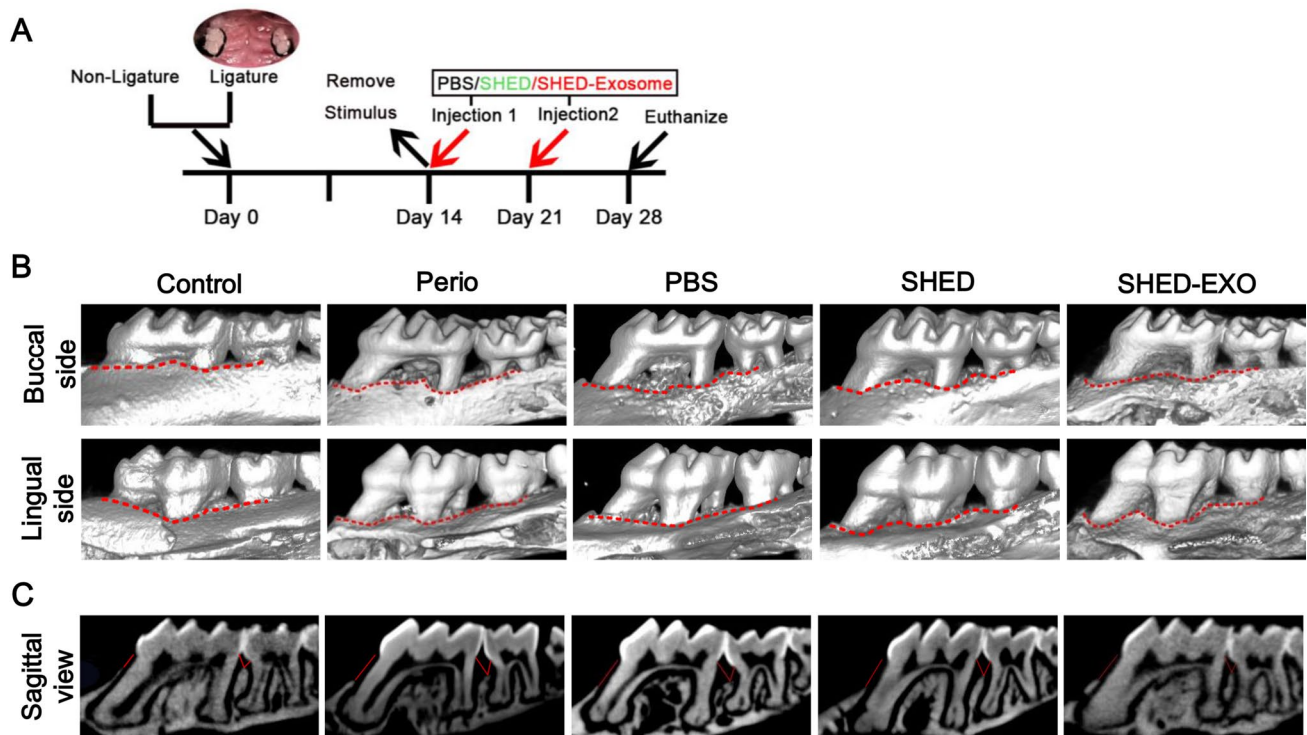
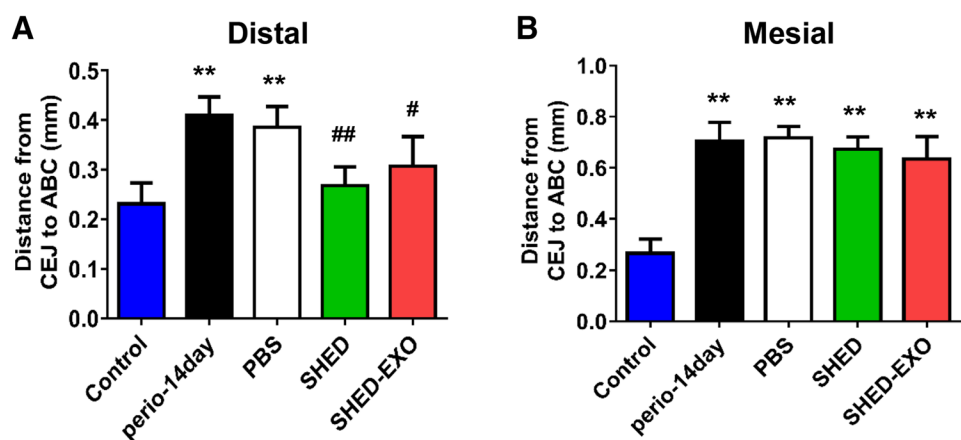


**Fig. 2** SHED possessed a stronger tissue regeneration ability than exosomes in periodontitis. **a** Schematic showing the procedures of periodontitis establishment and the following treatments with PBS, SHED, and SHED-Exo. **b** Reconstructed 3D micro-CT images of the upper jaw from the buccal and lingual sides in different groups. The red dotted line indicates the alveolar bone border. **c** Sagittal images of

the upper jaw displaying the distance from the cementoenamel junction (CEJ) to the alveolar bone crest (ABC), indicating the bone loss and degree of recovery after ligature-induced periodontitis. The red line shows the distance from the CEJ to the ABC of the mesial and distal sides of the first molar. (Color figure online)

**Fig. 3** Quantification of the degree of bone recovery. Histograms showing the quantitative analysis of the distance from the cementoenamel junction (CEJ) to the alveolar bone crest (ABC) on the distal and mesial sides of the first molar ( $n=4-6$  in each group).  $*P < 0.05$ ,  $**P < 0.01$  versus the healthy control group;  $\#P < 0.05$ ,  $\#\#P < 0.01$  versus the periodontitis group, as analyzed by one-way ANOVA followed by Tukey's post hoc test. Error bars indicate SD



the CEJ to the middle root level decreased, and adjacent gingival tissue showed obvious invagination (Fig. 4a, b). After the ligature was removed, upon PBS treatment, the alveolar bone could recover to a certain degree, reaching the upper root level (Fig. 4c). The bone crest level was more elevated in the SHED and SHED-Exo groups and almost recovered to the pre-periodontitis status (Fig. 4d, e). The gingival tissue was also reconstituted in these two

groups. Masson staining showed newly formed organized collagen fibers (blue color) in the SHED and SHED-Exo groups (Fig. 4i, j), as well as in the healthy control group (Fig. 4f). In the PBS treatment group, bundle-shaped fibers were not observed (Fig. 4g, h). Collectively, these data suggest that both SHED and SHED-Exo ameliorate periodontitis bone loss.

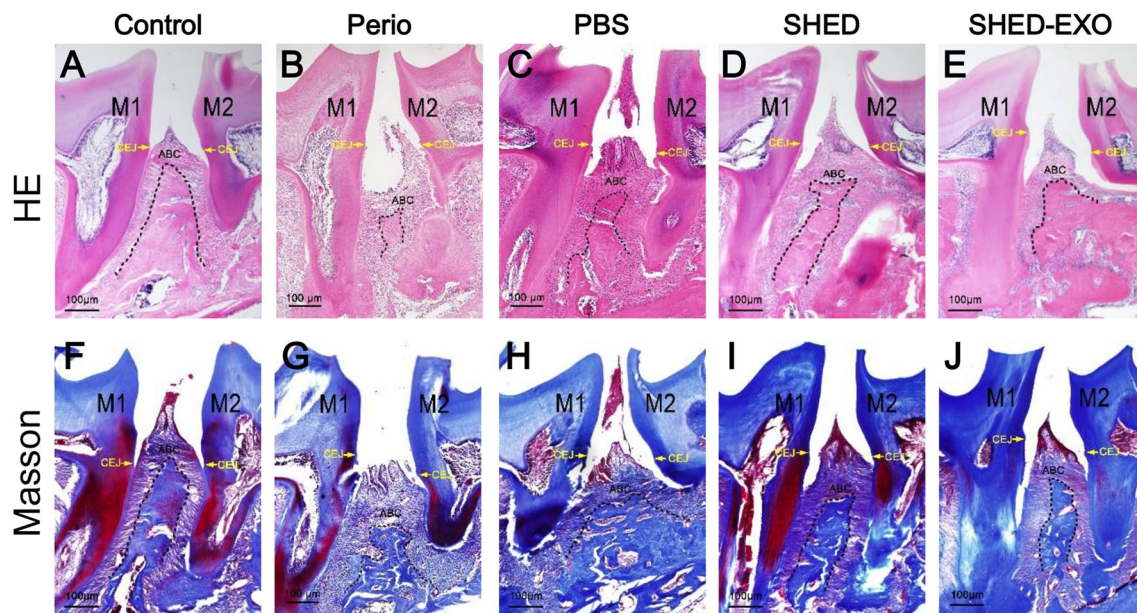


**Fig. 4** SHED-Exo promoted bone formation in vivo. **a–e** Representative histological sections of the alveolar bone between the first molar (M1) and the second molar (M2) stained with H&E. The black dotted

line indicates the height of the alveolar bone crest. **f–j** Masson staining showing the newly formed periodontal ligament collagen fibers in different groups

### SHED-Exo mildly promoted BMSCs proliferation and did not inhibit apoptosis

To analyze whether SHED-Exo promote bone regeneration by stimulating cell proliferation or inhibiting apoptosis, we examined the effects of SHED-Exo and SHED-CM on mouse BMSCs by supplementing the culture medium with PBS, SHED-Exo (1  $\mu\text{g}/\text{ml}$ ), or SHED-CM. BMSCs grew slowly at the beginning. On day 3, the absorbance of the SHED-Exo group was significantly higher than that of the PBS group, indicating SHED-Exo affect cell proliferation. From day 5, cells treated with SHED-CM started to grow

more robustly than those treated with PBS, and even more robustly than those treated with SHED-Exo ( $P < 0.05$ ; Fig. 5a). Therefore, SHED-Exo mildly increased the cell proliferation rate, but not as strongly as SHED-CM.

Apoptosis was examined by flow cytometry. Culture medium was supplemented with PBS, SHED-Exo (1  $\mu\text{g}/\text{ml}$ ), or SHED-CM for 24 h. On day 2, camptothecin was added to the BMSCs for 3 h to induce the early stage of apoptosis, which can be recognized with positive Annexin V and negative PI staining (Fig. 5b). SHED-Exo and SHED-CM decreased the proportion of apoptotic cells from 32.37% to 23.9% and 22.43%, respectively; for SHED-CM, this reduction was statistically significant.

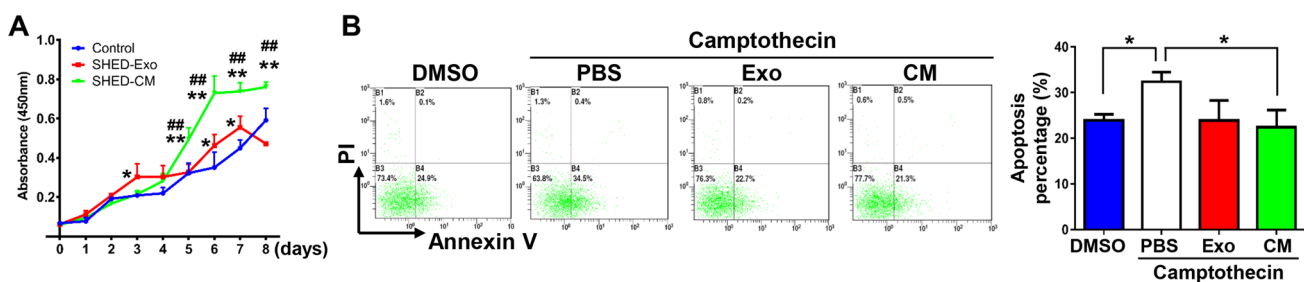


**Fig. 5** SHED-Exo increased BMSC proliferation. **a** The proliferation rate of BMSCs was measured daily from day 1 to day 8. Both SHED-Exo and SHED-CM promoted cell proliferation. \* $P < 0.05$ , \*\* $P < 0.01$  versus the control group; # $P < 0.05$ , ## $P < 0.01$  versus the SHED-Exo group, as analyzed by two-way ANOVA followed by

Tukey's post hoc test. Error bars indicate SD. **b** In vitro pre-treatment with SHED-Exo did not affect the percentage of early apoptotic cells. \* $P < 0.05$ , as analyzed by one-way ANOVA followed by Tukey's post hoc test. Error bars indicate SD

## SHED-Exo specifically induced BMSC osteogenesis and reduced the adipogenic ability

We further analyzed the effects of SHED-Exo on the osteogenic differentiation potential of stem cells. BMSCs were cultured in either culture medium (Ctrl) or osteogenic medium (OM) supplemented with PBS, SHED-Exo (1  $\mu\text{g/ml}$ ), or SHED-CM. After 3 days, *Alp* and *Runx2*

mRNA levels were increased in the SHED-CM group; no significant change was observed between the SHED-Exo and PBS groups (Fig. 6a). After osteogenic induction for 7 days, SHED-Exo started to exhibit its effects on osteogenesis. Alkaline phosphatase activity was significantly upregulated in the SHED-Exo and SHED-CM groups (Fig. 6b). Moreover, after 14 days of osteogenic induction, BMSCs differentiated into osteoblasts that formed mineral

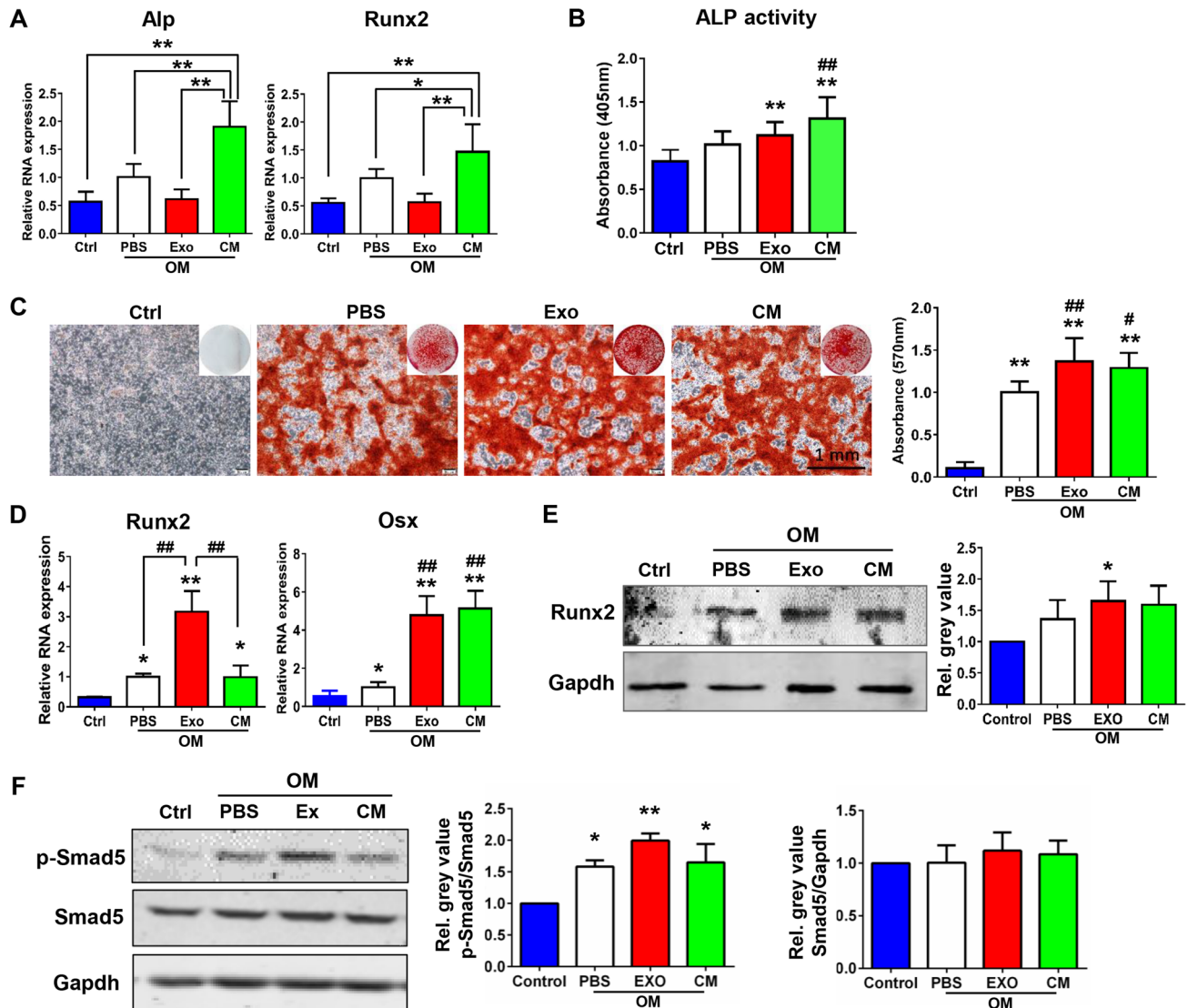


**Fig. 6** SHED-Exo promoted osteogenic differentiation in BMSCs. **a** mRNA levels of *Alp* and *Runx2* in BMSCs cultured in culture medium (Ctrl) or osteogenic medium (OM) supplemented with PBS, SHED-Exo, or SHED-CM on day 3, as analyzed by qRT-PCR. Data are normalized to *Gapdh* ( $n=4$ ).  $*P<0.05$ ,  $**P<0.01$ . **b** Histogram showing ALP activity on day 7 of different treatments ( $n=4-6$ ).  $*P<0.05$ ,  $**P<0.01$  versus the Ctrl group;  $\#P<0.05$ ,  $\#\#P<0.01$  versus the OM PBS group. **c** Representative images and quantification of Alizarin Red staining of BMSCs treated with SHED-Exo or SHED-CM ( $n=6-8$ ).  $*P<0.05$ ,  $**P<0.01$  versus the Ctrl group;  $\#P<0.05$ ,  $\#\#P<0.01$  versus the OM PBS group. **d** *Runx2* and *Osx* mRNA lev-

els were measured by qRT-PCR on day 14. Data are normalized to *Gapdh* ( $n=4$ ).  $*P<0.05$ ,  $**P<0.01$  versus the Ctrl group;  $\#P<0.05$ ,  $\#\#P<0.01$  versus the OM PBS group. **e** Western blot showing protein levels of Runx2 in differently treated cells and quantification of the gray signal intensity.  $*P<0.05$  versus the Ctrl group, as analyzed by one-way ANOVA followed by Tukey's post hoc test. Error bars indicate SD. **f** Western blot analysis showing protein levels of Smad5 and p-Smad5 in differently treated cells and quantification of the gray signal intensity.  $*P<0.05$ ,  $**P<0.01$  versus the Ctrl group, as analyzed by one-way ANOVA followed by Tukey's post hoc test. Error bars indicate SD



nodules (Fig. 6c) and exhibited strong expression of the osteogenesis-related marker genes *Runx2* and *Osx* at the mRNA and protein levels (Fig. 6d, e). As the time passed, the SHED-Exo group showed stronger mineral nodule formation potential and *Runx2* expression than the SHED-CM group. To investigate the underlying mechanisms of the role of exosomes in osteogenic differentiation, we examined the key factors in the transforming growth factor (TGF)- $\beta$  signaling pathway, which is closely involved in osteogenic differentiation and bone metabolism. Western blot analysis showed that p-Smad5 was activated in the presence of exosomes (Fig. 6f). Collectively, these results

indicate that SHED-Exo are capable of inducing osteogenic differentiation in BMSCs.

Since BMSCs have multi-differentiation abilities, we also cultured BMSCs in adipogenic medium supplemented with PBS, SHED-Exo, or SHED-CM for 14 days and observed the accumulation of lipid droplets and measured the mRNA expression levels of peroxisome proliferator-activated receptor  $\gamma$  (*PPAR $\gamma$* ). Surprisingly, lipid droplets were fewer and smaller in the SHED-Exo and SHED-CM groups than in the PBS group (Fig. 7a, b). mRNA levels of *PPAR $\gamma$*  confirmed that SHED-Exo and SHED-CM significantly decrease adipogenic differentiation in BMSCs (Fig. 7c). Collectively, these

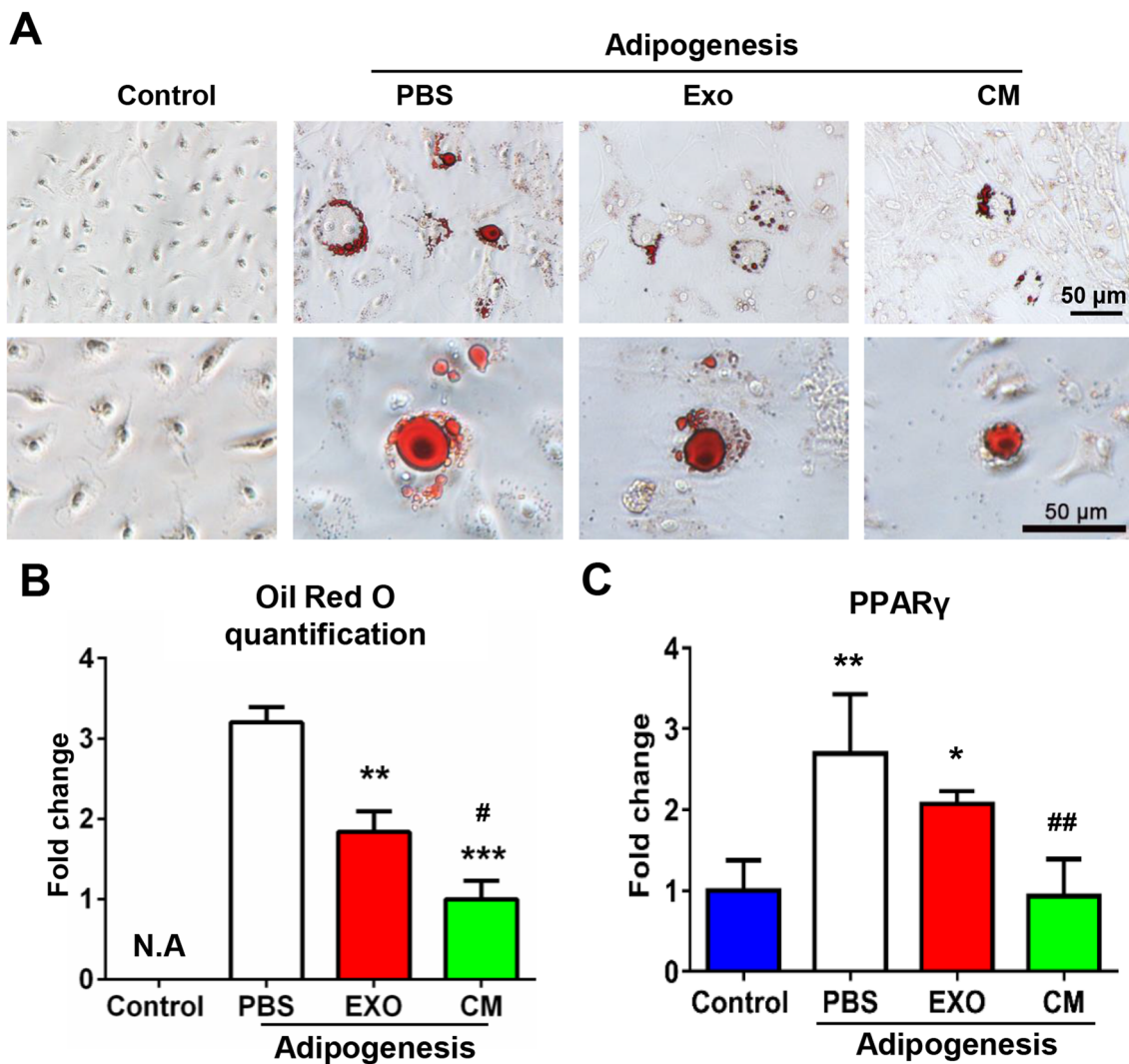


**Fig. 7** SHED-Exo inhibited the adipogenic potential of BMSCs. **a** Representative images of cells stained with Oil Red O after culturing in culture medium (Control) or adipogenic medium supplemented with PBS, SHED-Exo, or SHED-CM for 14 days. **b** Quantification of Oil Red O staining of BMSCs treated with SHED-Exo or SHED-CM ( $n=3-4$ ). \*\* $P<0.01$ , \*\*\* $P<0.001$  versus the Control group;

# $P<0.05$  versus the Adipogenesis PBS group. **c** mRNA levels of *PPAR $\gamma$*  in cells treated with SHED-Exo or SHED-CM for 14 days, as analyzed by qRT-PCR. Data are normalized to *GAPDH* ( $n=4$ ). \* $P<0.05$ , \*\* $P<0.01$  versus the Control group; ## $P<0.01$  versus the Adipogenesis PBS group, as analyzed by one-way ANOVA followed by Tukey's post hoc test. Error bars indicate SD



results indicate that SHED-Exo could promote osteogenic, but not adipogenic differentiation in BMSCs.

### SHED-Exo repressed the expression of inflammatory cytokines

SHED were previously demonstrated to have immunomodulatory functions (Yamaza et al. 2010). We speculated that SHED-Exo could modulate the immune reaction of their cells of origin. BMSCs were simulated with LPS (1  $\mu\text{g}/\text{ml}$ ) for 24 h. The mRNA levels of inflammation-related genes were analyzed by qRT-PCR. SHED-Exo and SHED-CM could significantly decrease *IL-6* and *TNF- $\alpha$*  expression (Fig. 8a). High concentrations of SHED-Exo (10  $\mu\text{g}/\text{ml}$ ) had opposite effects, increasing *IL-6* and *TNF- $\alpha$*  expression (Fig. 8b), which may enhance inflammation. Representative immunohistochemistry staining of *TNF- $\alpha$*  in periodontal defect areas (Supplementary Figure S1a–d), the area between the first and second molars, showed that SHED-Exo group could decrease the expression level of *TNF- $\alpha$*  after two weeks of treatment.

### Discussion

Here, we characterized SHED-Exo and evaluated whether they possess similar functions as their cells of origin, including stimulating cell proliferation, promoting osteogenesis, modulating inflammation, and increasing the regeneration of bone tissue in vivo. Although SHED-Exo did not enhance the multi-differentiation potential of BMSCs (e.g., SHED-Exo did not stimulate adipogenic differentiation, which is related to bone ageing and is a risk factor for osteoporosis), they promoted the transcription of osteogenesis-related

genes and the formation of mineralized bone tissue. Based on these findings, we speculate that SHED-Exo might be a valuable source for bone regeneration therapies.

It has been established that extracellular vesicles, exosomes, and microvesicles are released by virtually all types of cells and mediate cell–cell communications. However, SHED-Exo have not yet been investigated. First, we characterized SHED-Exo and showed that their shape, size, and protein markers were consistent with those of exosomes of mesenchymal cell origin (Huang et al. 2016; Jiang et al. 2017). We wish to emphasize that SHED, in contrast to other types of stem cells, are easily accessible, have a strong stem cell potential, and exhibit a stable telomerase expression (Seo et al. 2008), even after cryopreservation (Ma et al. 2012). In this study, BMSCs treated with SHED-CM exhibited robust proliferation, which was  $\sim 50\%$  higher than in the PBS group and  $\sim 30\%$  higher than in the SHED-Exo group since day 5. SHED-CM also exhibited significant effects on the proportion of early apoptotic cells; these effects were slightly stronger than those of SHED-Exo. Studies have also proved that SHED are able to induce bone formation, repair refractory neural injuries (Yamagata et al. 2013), and elevate the ratio of regulatory T cells (Yamaza et al. 2010). Moreover, SHED are not ethically controversial and easily accessible, and their collection is easy, painless, and noninvasive. Under the mechanical force exerted by the erupting permanent tooth, the deciduous tooth crown, where SHED are maintained in the living pulp, exfoliate ultimately (Wu et al. 2020). Thus, exfoliated deciduous teeth could be a feasible cell source for cell-based therapy and an ideal source for exosome production.

Exosomes have been reported to participate in cancer progression (Zhang et al. 2015), immune modulation (Milane et al. 2015), neural degeneration (Zhang and Yang 2018),

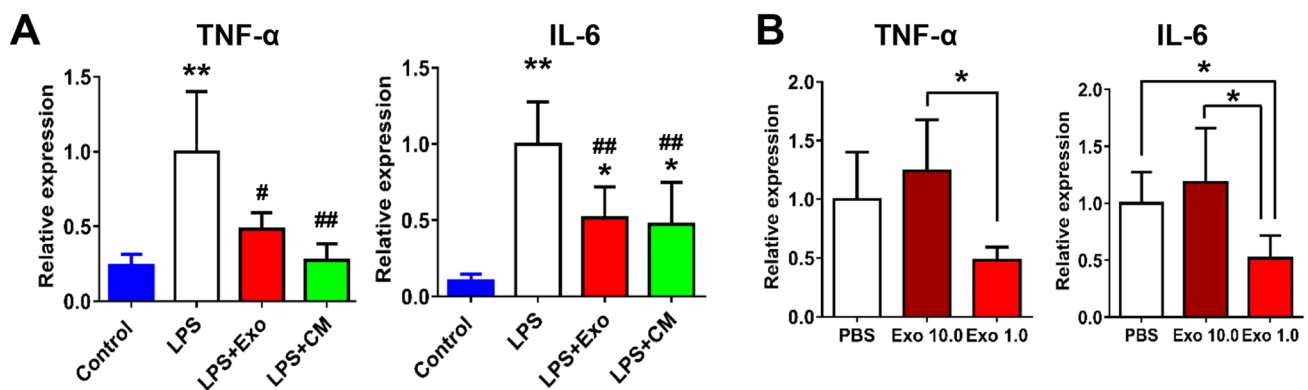


**Fig. 8** Low doses of exosomes inhibited inflammation. **a** Relative mRNA levels of the inflammation-related genes *TNF- $\alpha$*  and *IL-6* in BMSCs treated with exosomes (Exo) or conditioned medium (CM), as analyzed by qRT-PCR. Data are normalized to *Gapdh*. \* $P < 0.05$ , \*\* $P < 0.01$  versus the control group; # $P < 0.05$ , ## $P < 0.01$  versus the

LPS group. **b** mRNA levels of *TNF- $\alpha$*  and *IL-6* in BMSCs treated with PBS, exosomes (10.0  $\mu\text{g}/\text{ml}$ ), or exosomes (1.0  $\mu\text{g}/\text{ml}$ ) in the presence of LPS ( $n = 4$ ). \* $P < 0.05$ , as analyzed by one-way ANOVA followed by Tukey's post hoc test. Error bars indicate SD

cell differentiation (Mao et al. 2018), and organ development (Hayashi and Hoffman 2017; Jiang et al. 2017). In the bone metabolism environment, it has been shown that pre-osteoblast-derived exosomes promote BMSC differentiation into osteoblasts (Cui et al. 2016), and exosomes from myoblasts could enhance osteogenic differentiation of pre-osteoblasts (Xu et al. 2018). Because exosomes can stimulate osteogenesis or angiogenesis, specific exosomes have been utilized in the treatment of osteonecrosis and fractures (Fang et al. 2019; Zhang et al. 2019). In this study, we demonstrated that exosomes from SHED could promote osteogenic differentiation in BMSCs. SHED-Exo were injected as a therapeutic tool to treat periodontitis *in vivo*, and we found that alveolar bone loss was restored to similar levels to the healthy control group. Periodontal ligament fibers, which are key elements in the regulation of the periodontal microenvironment, had a bundle-like structure after SHED or SHED-Exo treatment, as shown by Masson staining. However, in the mesial bone resorption area, neither SHED nor SHED-Exo could restore alveolar bone loss. An important factor is the anatomical bone structure of the mesial root, which has a gentle slope and a thin bony land, as shown in Fig. 2b. As a result, it is hard to form a bony pocket in the mesial space, as seen in the distal part, to restrain injected cells or exosomes from flowing away. Gel-like scaffolds can be applied with SHED-Exo in further studies to maintain extracellular vesicles in the bone defect area. We performed *in vitro* experiments to corroborate the results from the mouse model. Alkaline phosphatase activity, Alizarin Red staining, and mRNA levels of osteogenesis-related genes indicated that the ability of SHED-Exo to stimulate osteogenic differentiation is superior to that of SHED-CM. Application of SHED-CM for 3 days showed a higher efficiency in the early induction of osteogenic commitment, while SHED-Exo did not. In previous studies (Tian et al. 2014), it was shown that cells internalize exosomes via membrane fusion or endocytosis, which may delay the biological functions stimulated by exosomes compared with conditioned medium. We cannot exclude other possibility that other biological mechanisms cause this difference in the early stage, which requires further study. To explore the underlying mechanism, we tested the TGF- $\beta$  signaling plays, which has been well known in the development and maintenance of bone metabolism (Urist 1965). After stimulation with SHED-Exo, p-Smad5 levels were significantly upregulated. It has been proved that Runx2 is a target of TGF- $\beta$  signaling, and cooperation between Runx2 and Smad5 induces the expression of osteoblast-specific genes. Collectively, we conclude that SHED-Exo participate in Smad5/Runx2 signaling and activate osteogenic differentiation in BMSCs. This finding was supported by another study discussing SHED-Exo effects on periodontal ligament stem cells (PDLSCs). PDLSCs are a major component of periodontal structures and could be induced to

express osteogenic markers with SHED-Exo stimulation through BMP and WNT signaling pathway (Wang et al. 2020). The bone recovery results we observed in mice periodontal disease experiments, may not only contribute to BMSCs osteogenic differentiation induced by SHED-Exo, but also to PDLSCs osteogenesis process.

Interestingly, when we analyzed the adipogenic differentiation of BMSCs, SHED-Exo and SHED-CM showed inhibitory effects, as lipid droplets were fewer and smaller, and the expression of adipogenesis-related genes was inhibited. BMSCs can be progenitors of both osteoblasts and adipocytes. SHED-Exo and SHED-CM enhance osteogenic differentiation in BMSCs at the expense of adipogenic differentiation; the underlying mechanisms will require further exploration.

Additionally, previous studies focused on the application of SHED in the treatment of immune disease, such as systemic lupus erythematosus (Yamaza et al. 2010), and to alleviate hyposalivation caused by Sjogren syndrome (Du et al. 2019). SHED-CM suppressed the expression of pro-inflammatory cytokines, iNOS, and 3-nitrotyrosine and improved the cognitive function of mice (Yamamoto et al. 2014). We speculate that SHED-Exo may also carry genetic information and participate in immunomodulation, as their parent cells. Exosomes may have both pro- and anti-inflammatory properties and participate in different stages of the inflammatory response, communicating with macrophages, (Li et al. 2016) neutrophils, (Liu et al. 2016) microglia, (Li et al. 2019) and epithelial cells (Shao et al. 2019), among others. In this animal study, the expression level of TNF- $\alpha$  in the periodontal defect area was reduced after two-week treatment of SHED and SHED-Exo. After inducing inflammation with LPS *in vitro*, we showed that SHED-Exo and SHED-CM could significantly inhibit the expression of pro-inflammatory cytokines. Similarly to growth factors, the therapeutic effects of exosomes are dose-dependent within a certain range. For example, endothelial cell-derived exosomes promoted angiogenesis in a dose-dependent manner (Nooshabadi et al. 2019). We founded that high concentrations of SHED-Exo (10  $\mu\text{g/ml}$ ) had opposite effects, which is consistent with a previous study (Smyth et al. 2015). There are few studies on the toxicity of exosomes. One side effect was reported by a study in which 200  $\mu\text{g}$  of exosomes was injected into mice. (Smyth et al. 2015) The mechanisms underlying the dose-dependent effects of SHED-Exo on inflammation need further investigation.

In comparison with stem cell transplantation, exosome treatment, a cell-free therapeutic tool, has several advantages. Exosomes are derived from endocytic compartments, and hence, avoid the toxicity and immunogenicity issues raised by biomaterial treatment (Fleury et al. 2014). They have better endocytosis ability, immunogenicity, and especially innate biocompatibility (Heusermann et al. 2016; Tian

et al. 2013). Therefore, they have been utilized as promising tools for drug delivery and gene therapy (Pitt et al. 2016; Usman et al. 2018) for multiple diseases, such as Alzheimer's disease (Alvarez-Erviti et al. 2011) and cancer (Liang et al. 2019), and in tissue regeneration (Huang et al. 2016). Furthermore, exosomes are very stable and can be stored for approximately 6 months without loss of potency (Chaput et al. 2004).

The therapeutic effects of exosomes have been discovered because their content, including signaling proteins, lipids, nucleic acids, and metabolites, can be transported to target cells and activate downstream signaling pathways. The main limitation of this study lies in the fact that we did not include an analysis of the signals or components transferred from exosomes to target cells. Further experiments will be needed to unveil the underlying mechanisms of the observed effects of exosomes.

In summary, the present data are consistent with our hypothesis that the osteogenic capability of BMSCs is enhanced by SHED-Exo. Our results improve our understanding of the mechanisms by which SHED transplantation stimulates tissue regeneration and of the potential to utilize exosomes as a cell-free therapeutic strategy to treat periodontitis and other bone diseases.

**Author contributions** JW contributed to study design, data collection, statistical analysis and data interpretation; YS and ZD contributed to data collection and data interpretation; FY contributed to literature search; YZ contributed to exosomes collection and data collection and fund collection; NJ contributed to manuscript preparation and funds collection. NJ and XG contributed to study design, statistical analysis, data interpretation and manuscript revision. All authors approved the final version of the manuscript.

**Funding** This study was financially supported by grants from the National Natural Science Foundation of China Nos. 81970901(N.J.), 81600820(N.J) and 81801014 (Y.Z).

**Data availability** The authors declare that the data supporting the findings of this study are available within the manuscript and the supplementary materials.

## Compliance with ethical standards

**Conflict of interest** The authors have no conflicts of interest to declare.

**Ethical approval** Protocols were approved by the Peking University Ethical Committee (LA2019148).

## References

Abe T, Hajishengallis G (2013) Optimization of the ligature-induced periodontitis model in mice. *J Immunol Methods* 394(1–2):49–54

- Alvarez-Erviti L, Seow Y, Yin H, Betts C, Lakkhal S, Wood MJ (2011) Delivery of siRNA to the mouse brain by systemic injection of targeted exosomes. *Nat Biotechnol* 29(4):341–345
- Bianco P, Cao X, Frenette PS, Mao JJ, Robey PG, Simmons PJ et al (2013) The meaning, the sense and the significance: translating the science of mesenchymal stem cells into medicine. *Nat Med* 19(1):35–42
- Catalano M, O'Driscoll L (2020) Inhibiting extracellular vesicles formation and release: a review of EV inhibitors. *J Extracell Vesicles* 9(1):1703244
- Chaput N, Taieb J, Scharz NE, Andre F, Angevin E, Zitvogel L (2004) Exosome-based immunotherapy. *Cancer Immunol Immunother* 53(3):234–239
- Cui Y, Luan J, Li H, Zhou X, Han J (2016) Exosomes derived from mineralizing osteoblasts promote ST2 cell osteogenic differentiation by alteration of microRNA expression. *FEBS Lett* 590(1):185–192
- Du ZH, Li SL, Ge XY, Yu GY, Ding C (2018) Comparison of the secretory related molecules expression in stem cells from the pulp of human exfoliated deciduous teeth and dental pulp stem cells. *Zhonghua Kou Qiang Yi Xue Za Zhi* 53(11):741–747
- Du ZH, Ding C, Zhang Q, Zhang Y, Ge XY, Li SL et al (2019) Stem cells from exfoliated deciduous teeth alleviate hyposalivation caused by Sjogren syndrome. *Oral Dis* 25(6):1530–1544
- Fang SH, Li YF, Chen P (2019) Osteogenic effect of bone marrow mesenchymal stem cell-derived exosomes on steroid-induced osteonecrosis of the femoral head. *Drug Des Dev Therapy* 13:45–55
- Fitts CA, Ji N, Li Y, Tan C (2019) Exploiting exosomes in cancer liquid biopsies and drug delivery. *Adv Healthc Mater* 8(6):e1801268
- Fleury A, Martinez MC, Le Lay S (2014) Extracellular vesicles as therapeutic tools in cardiovascular diseases. *Front Immunol* 5:370
- Haniffa MA, Collin MP, Buckley CD, Dazzi F (2009) Mesenchymal stem cells: the fibroblasts' new clothes? *Haematologica* 94(2):258–263
- Hayashi T, Hoffman MP (2017) Exosomal microRNA communication between tissues during organogenesis. *RNA Biol* 14(12):1683–1689
- Heusermann W, Hean J, Trojer D, Steib E, von Bueren S, Graff-Meyer A et al (2016) Exosomes surf on filopodia to enter cells at endocytic hot spots, traffic within endosomes, and are targeted to the ER. *J Cell Biol* 213(2):173–184
- Huang CC, Narayanan R, Alapati S, Ravindran S (2016) Exosomes as biomimetic tools for stem cell differentiation: applications in dental pulp tissue regeneration. *Biomaterials* 111:103–115
- Jiang N, Xiang L, He L, Yang G, Zheng J, Wang C et al (2017) Exosomes mediate epithelium-mesenchyme crosstalk in organ development. *ACS Nano* 11(8):7736–7746
- Kalluri R, LeBleu VS (2020) The biology, function, and biomedical applications of exosomes. *Science* 367:6478
- Lee HS, Jeon M, Kim SO, Kim SH, Lee JH, Ahn SJ et al (2015) Characteristics of stem cells from human exfoliated deciduous teeth (SHED) from intact cryopreserved deciduous teeth. *Cryobiology* 71(3):374–383
- Li X, Liu LY, Yang J, Yu YH, Chai JK, Wang LY et al (2016) Exosome derived from human umbilical cord mesenchymal stem cell mediates MiR-181c attenuating burn-induced excessive inflammation. *Ebiomedicine* 8:72–82
- Li ZJ, Liu F, He X, Yang X, Shan FP, Feng J (2019) Exosomes derived from mesenchymal stem cells attenuate inflammation and demyelination of the central nervous system in EAE rats by regulating the polarization of microglia. *Int Immunopharmacol* 67:268–280
- Liang QL, Bie NN, Yong TY, Tang K, Shi XL, Wei ZH et al (2019) The softness of tumour-cell-derived microparticles regulates their drug-delivery efficiency. *Nat Biomed Eng* 3(9):729–740
- Liu YF, Gu Y, Han YM, Zhang Q, Jiang ZP, Zhang X et al (2016) Tumor exosomal RNAs promote lung pre-metastatic niche



- formation by activating alveolar epithelial TLR3 to recruit neutrophils. *Cancer Cell* 30(2):243–256
- Ma L, Makino Y, Yamaza H, Akiyama K, Hoshino Y, Song GT et al (2012) Cryopreserved dental pulp tissues of exfoliated deciduous teeth is a feasible stem cell resource for regenerative medicine. *PLoS ONE* 7:e51777
- Mao G, Zhang Z, Hu S, Chang Z, Huang Z, Liao W et al (2018) Exosomes derived from miR-92a-3p-overexpressing human mesenchymal stem cells enhance chondrogenesis and suppress cartilage degradation via targeting WNT5A. *Stem Cell Res Ther* 9(1):247
- Mathieu M, Martin-Jaulier L, Lavieu G, Thery C (2019) Specificities of secretion and uptake of exosomes and other extracellular vesicles for cell-to-cell communication. *Nat Cell Biol* 21(1):9–17
- Milane L, Singh A, Mattheolabakis G, Suresh M, Amiji MM (2015) Exosome mediated communication within the tumor microenvironment. *J Control Release* 219:278–294
- Miura M, Gronthos S, Zhao M, Lu B, Fisher LW, Robey PG et al (2003a) SHED: stem cells from human exfoliated deciduous teeth. *Proc Natl Acad Sci USA* 100(10):5807–5812
- Miura M, Gronthos S, Zhao MR, Lu B, Fisher LW, Robey PG et al (2003b) SHED: Stem cells from human exfoliated deciduous teeth. *Proc Natl Acad Sci USA* 100(10):5807–5812
- Nooshabadi VT, Verdi J, Ebrahimi-Barough S, Mowla J, Atlasi MA, Mazoochi T et al (2019) Endometrial mesenchymal stem cell-derived exosome promote endothelial cell angiogenesis in a dose dependent manner: a new perspective on regenerative medicine and cell-free therapy. *Archiv Neurosci* 6(4):24–29
- Pitt JM, Kroemer G, Zitvogel L (2016) Extracellular vesicles: masters of intercellular communication and potential clinical interventions. *J Clin Invest* 126(4):1139–1143
- Seo BM, Sonoyama W, Yamaza T, Coppe C, Kikui T, Akiyama K et al (2008) SHED repair critical-size calvarial defects in mice. *Oral Dis* 14(5):428–434
- Shao S, Fang H, Zhang JL, Jiang M, Xue K, Ma JY et al (2019) Neutrophil exosomes enhance the skin autoinflammation in generalized pustular psoriasis via activating keratinocytes. *Faseb J* 33(6):6813–6828
- Smyth T, Kullberg M, Malik N, Smith-Jones P, Graner MW, Anchordouy TJ (2015) Biodistribution and delivery efficiency of unmodified tumor-derived exosomes. *J Control Release* 199:145–155
- Taguchi T, Yanagi Y, Yoshimaru K, Zhang XY, Matsuura T, Nakayama K et al (2019) Regenerative medicine using stem cells from human exfoliated deciduous teeth (SHED): a promising new treatment in pediatric surgery. *Surg Today* 49(4):316–322
- Tian T, Zhu YL, Hu FH, Wang YY, Huang NP, Xiao ZD (2013) Dynamics of exosome internalization and trafficking. *J Cell Physiol* 228(7):1487–1495
- Tian T, Zhu YL, Zhou YY, Liang GF, Wang YY, Hu FH et al (2014) Exosome Uptake through Clathrin-mediated Endocytosis and Macropinocytosis and Mediating miR-21 Delivery. *J Biol Chem* 289(32):22258–22267
- Urist MR (1965) Bone: formation by autoinduction. *Science* 150(3698):893–899
- Usman WM, Pham TC, Kwok YY, Vu LT, Ma V, Peng B et al (2018) Efficient RNA drug delivery using red blood cell extracellular vesicles. *Nat Commun* 9(1):2359
- Wang M, Li J, Ye Y, He S, Song J (2020) SHED-derived conditioned exosomes enhance the osteogenic differentiation of PDLSCs via Wnt and BMP signaling in vitro. *Differentiation* 111:1–11
- Wu X, Hu J, Li G, Li Y, Zhang J, Wang F et al (2020) Biomechanical stress regulates mammalian tooth replacement via the integrin beta1-RUNX2-Wnt pathway. *EMBO J* 39(3):e102374
- Xu Q, Cui YZ, Luan J, Zhou XY, Li HY, Han JX (2018) Exosomes from C2C12 myoblasts enhance osteogenic differentiation of MC3T3-E1 pre-osteoblasts by delivering miR-27a-3p. *Biochem Biophys Res Commun* 498(1):32–37
- Yamagata M, Yamamoto A, Kako E, Kaneko N, Matsubara K, Sakai K et al (2013) Human dental pulp-derived stem cells protect against hypoxic-ischemic brain injury in neonatal mice. *Stroke* 44(2):551–554
- Yamamoto A, Sakai K, Matsubara K, Kano F, Ueda M (2014) Multifaceted neuro-regenerative activities of human dental pulp stem cells for functional recovery after spinal cord injury. *Neurosci Res* 78:16–20
- Yamaza T, Kentaro A, Chen C, Liu Y, Shi Y, Gronthos S et al (2010) Immunomodulatory properties of stem cells from human exfoliated deciduous teeth. *Stem Cell Res Ther* 1(1):5
- Yuan Y, Du W, Liu J, Ma W, Zhang L, Du Z et al (2018) Stem cell-derived exosome in cardiovascular diseases: macro roles of micro particles. *Front Pharmacol* 9:547
- Zhang G, Yang P (2018) A novel cell-cell communication mechanism in the nervous system: exosomes. *J Neurosci Res* 96(1):45–52
- Zhang L, Zhang S, Yao J, Lowery FJ, Zhang Q, Huang WC et al (2015) Microenvironment-induced PTEN loss by exosomal microRNA primes brain metastasis outgrowth. *Nature* 527(7576):100–104
- Zhang YT, Hao ZC, Wang PF, Xia Y, Wu JH, Xia DM et al (2019) Exosomes from human umbilical cord mesenchymal stem cells enhance fracture healing through HIF-1 alpha-mediated promotion of angiogenesis in a rat model of stabilized fracture. *Cell Prolif* 52(2):e12570

**Publisher's Note** Springer Nature remains neutral with regard to jurisdictional claims in published maps and institutional affiliations.